Hindawi
Wireless Communications and Mobile Computing
Volume 2020, Article ID 6669547, 8 pages
https://doi.org/10.1155/2020/6669547

Research Article

High-Precision Mutual Coupling Coefficient Estimation for Adaptive Beamforming

Ziang Feng,[1] **Guoping Hu**,[2] **Qichao Ge**,[1] **and Hao Zhou**[2]

[1]*Graduate College, Air Force Engineering University, Xi'an 710051, China*
[2]*Air and Missile Defense College, Air Force Engineering University, Xi'an 710051, China*

Correspondence should be addressed to Qichao Ge; geqichao927@163.com

Received 1 November 2020; Revised 2 December 2020; Accepted 13 December 2020; Published 21 December 2020

Academic Editor: Liangtian Wan

Here, a high-precision mutual coupling coefficient estimation method is proposed that is more suitable for adaptive beamforming than traditional algorithms. According to the relationship between the designed transition matrix and the signal, the proposed algorithm selects the transition matrix corresponding to the high-power signal. The high-precision estimation of the mutual coupling coefficient is obtained by using the selected transition matrix estimation, which yields relatively good estimation accuracy for the mutual coupling coefficient when the desired signal-to-noise ratio (SNR) is low and relatively robust adaptive beamforming with unknown mutual coupling. Simulation results demonstrate the validity of the proposed method.

1. Introduction

Signal processing technology, such as direction of arrival (DOA) and robust adaptive beamforming (RAB), has been widely used in radar, sonar, communication, etc. [1–7]. As a kind of array error, mutual coupling seriously affects the performance of various signal processing algorithms [8–11]. To avoid the influence of mutual coupling, a middle subarray-based (MSB) approach is proposed in [12], and a maximum interelement spacing constraint (MISC) array is designed in [13]. In addition, many algorithms for calibrating mutual coupling have been proposed. Since the mutual coupling matrix (MCM) can be modeled as a banded symmetric Toeplitz matrix for a uniform linear array (ULA), a subspace-based method is proposed in [14], and a fourth-order cumulant- (FOC-) based method is proposed in [15]. In addition, an iterative autocalibration algorithm based on the eigendecomposition of the sampling covariance matrix for a uniform circular array (UCA) is proposed to calibrate unknown mutual coupling since the MCM has a complex symmetric circular Toeplitz structure in a UCA in [16]. Furthermore, a joint DOA estimation and mutual coupling self-calibration for ULA-based bistatic multiple-input-multiple-output (MIMO) radar is proposed in [17]. Based on [16], a parameter estimation method for direction-dependent mutual coupling is proposed in [18]. However, the MSB approach reduces the degree of freedom (DOF) of the array, and the complex structure of the MISC array increases the difficulty of signal processing, while the subspace-based method in [14] constructs a high-dimensional matrix, and the algorithms proposed in [16, 18] both need an iterative process. To reduce the computational complexity in estimating mutual coupling, two low-complexity algorithms for direction-dependent mutual coupling and direction-independent mutual coupling were proposed in [19, 20], respectively.

To improve the robustness of adaptive beamforming in the presence of unknown mutual coupling, a middle subarray-plus-reconstruction-based (MSRB) method combining the MSB algorithm with interference-plus-noise covariance matrix (INCM) reconstruction [21] is proposed in [22]. However, the MSRB approach requires a large array aperture for high performance. Similarly, the desired signal steering vector with unknown mutual coupling is calibrated by using the specific structure of the MCM, and the new beamformer is obtained by combining a diagonal loading beamformer with the desired signal steering vector estimation [11]. To reduce the computational load, a subspace-plus-reconstruction-based (SRB) beamformer is then designed by

incorporating the subspace-based mutual coupling coefficient estimation method [14], and INCM reconstruction is designed in [10]. Obviously, the algorithms proposed in [20] can be utilized to design beamformers to further reduce the computational load. However, the algorithm proposed in [20] cannot obtain a high accuracy for the mutual coupling coefficients when there is a high power difference between signals since the accuracy of the subspace-based method is positively correlated with the signal-to-noise ratio (SNR).

To further improve the robustness of adaptive beamforming to unknown mutual coupling, a novel subspace-based algorithm is proposed to estimate mutual coupling coefficients and is utilized to design a novel adaptive beamformer. Different from the algorithms proposed in [20], we add the process of selecting several suitable transitional matrices and calculating their inverses. After estimating a group of transitional matrices, we select the transitional matrix corresponding to the maximum spectral peak to estimate the mutual coupling coefficient vector and the MCM. Then, the signal steering vector is calibrated with the estimated MCM. Finally, by combining the estimated MCM and the INCM reconstruction, we propose a novel adaptive beamforming algorithm. According to simulation, compared with several existing approaches, the proposed mutual coupling estimation method has a higher estimation accuracy, especially in the case of SNR differences between several signals. The designed beamformer is more robust than the existing beamformer to mutual coupling.

2. Signal Mode

We assume that a ULA of N sensors is impinged by L narrowband uncorrelated signals, and the noise is additive white Gaussian noise. We assume that the signal and noise are statistically independent. When the direction-independent mutual coupling effect is considered, the received snapshot at the kth time instant can be expressed as

$$\mathbf{x}(k) = \mathbf{x}_s(k) + \mathbf{n}(k) = \mathbf{C}\sum_{l=1}^{L} s_l(k)\mathbf{a}(\theta_l) + \mathbf{n}(k), \tag{1}$$

where $\mathbf{x}_s(k)$ and $\mathbf{n}(k)$ stand for the $N \times 1$ vector of the signal and noise, respectively. θ_l is the lth signal DOA, and $s_l(k)$ and $\mathbf{a}(\theta_l) \in \mathbb{C}^{N\times 1}$ are the corresponding complex envelope and steering vector, respectively. $\mathbf{C} \in \mathbb{C}^{N\times N}$ denotes the MCM, which can be molded as a banded symmetric Toeplitz matrix for a ULA since the mutual coupling coefficients between the elements are inversely proportional to their distance. In general, we assume that the mutual coupling coefficient becomes zero when the spacing of two elements exceeds an interelement spacing of P; hence, the mutual coupling coefficient vector and the MCM can be defined as

$$\begin{aligned} \mathbf{c} &= [c_0, c_1, c_2, \cdots, c_{P-1}]^T, \\ \mathbf{C} &= \text{Toeplitz}(\mathbf{c}_N, \mathbf{c}_N), \end{aligned} \tag{2}$$

where $c_0 = 1$ and $\mathbf{c}_N = [\mathbf{c}^T, 0]^T \in \mathbb{C}^{N\times 1}$.

Recall that in Equation (1), the covariance matrix of $\mathbf{x}(k)$ can be given by

$$\mathbf{R} = E\left[\mathbf{x}(k)\mathbf{x}^H(k)\right] = \mathbf{C}\mathbf{A}\mathbf{R}_s\mathbf{A}^H\mathbf{C}^H + \sigma_n^2\mathbf{I}_N, \tag{3}$$

where $E[\cdot]$ and $(\cdot)^H$ represent the expectation and conjugate transpose, respectively. $\mathbf{A} = [\mathbf{a}_1, \mathbf{a}_2, \cdots, \mathbf{a}_L] \in \mathbb{C}^{N\times L}$ denotes the manifold matrix, and $\mathbf{R}_s = \text{diag}\,(\sigma_1^2, \sigma_2^2, \cdots, \sigma_L^2) \in \mathbb{R}^{L\times L}$ is the covariance matrix of signals, where σ_l^2 is the power of the l th signal. σ_n^2 is the power of the noise, and $\mathbf{I}_N \in \mathbb{R}^{N\times N}$ is an identity matrix.

In practice, the sampling covariance matrix is usually used in lieu of the covariance matrix, and the sampling covariance matrix $\widehat{\mathbf{R}}_x$ can be expressed as

$$\widehat{\mathbf{R}}_x = \frac{1}{K}\sum_{k=1}^{K}\mathbf{x}(k)\mathbf{x}^H(k), \tag{4}$$

where K stands for the number of snapshots. After eigendecomposing $\widehat{\mathbf{R}}_x$, we can obtain

$$\widehat{\mathbf{R}}_x = \mathbf{U}\mathbf{\Lambda}\mathbf{U}^H = \mathbf{U}_s\mathbf{\Lambda}_s\mathbf{U}_s^H + \mathbf{U}_n\mathbf{\Lambda}_n\mathbf{U}_n^H, \tag{5}$$

where $\mathbf{U}$ is the eigenvector matrix and $\mathbf{\Lambda}$ denotes the corresponding eigenvalue matrix. $\mathbf{\Lambda}_s$ and $\mathbf{\Lambda}_n$ are diagonal matrices that contain L large eigenvalues and the remaining small eigenvalues, respectively. $\mathbf{U}_s$ and $\mathbf{U}_n$ are the corresponding eigenvector matrices. In general, $\mathbf{U}_s$ is called the signal subspace, and $\mathbf{U}_n$ is called the noise subspace. Additionally, $\{\mathbf{C}\mathbf{a}(\theta_l)\}_{l=1}^{L}$ can span the signal subspace.

For instance, when DOA estimation is performed using a subspace algorithm, the spatial spectral function shown below is usually used [13]:

$$P(\theta) = \frac{1}{\mathbf{a}^H(\theta)\mathbf{U}_n\mathbf{U}_n^H\mathbf{a}(\theta)}. \tag{6}$$

Obviously, if the MCM is unknown, the spectral peaks do not correspond to the true DOA of the signals since $\mathbf{U}_n$ is orthogonal to $\mathbf{C}\mathbf{a}(\theta)$, not $\mathbf{a}(\theta)$. That is, if $\mathbf{C}$ can be estimated, then the DOA of signals can be estimated.

3. Proposed Algorithm

3.1. Mutual Coupling Coefficient Estimation. According to the banded symmetric Toeplitz structure of MCM $\mathbf{C}$, we can obtain [19]

$$\mathbf{C}\mathbf{a}(\theta) = \mathbf{T}(\theta)\mathbf{c}, \tag{7}$$

where

$$\mathbf{T}(\theta) = [\mathbf{E}_1\mathbf{a}(\theta), \mathbf{E}_2(\theta)\mathbf{a}(\theta), \cdots, \mathbf{E}_P(\theta)\mathbf{a}(\theta)], \tag{8}$$

where

$$\left[\mathbf{E}_p\right]_{ij} = \begin{cases} 1, & \text{if}\left[\mathbf{C}\right]_{ij} = c_p \\ 0, & \text{otherwise} \end{cases}, \quad p = 0, 1, \cdots, P-1. \tag{9}$$

Based on the orthogonality between $\mathbf{Ca}(\theta_l)$ and the noise subspace $\mathbf{U}_\mathrm{n}$, we can obtain

$$\mathbf{a}^H(\theta_l)\mathbf{C}^H\mathbf{U}_n\mathbf{U}_n^H\mathbf{Ca}(\theta_l) = 0. \tag{10}$$

Recall that Equations (7) and (10) can be rewritten as

$$\mathbf{c}^H\mathbf{Q}(\theta_l)\mathbf{c} = 0, \tag{11}$$

where $\mathbf{Q}(\theta)$ is a transitional matrix and is defined as

$$\mathbf{Q}(\theta) = \mathbf{T}^H(\theta)\mathbf{U}_\mathrm{n}\mathbf{U}_\mathrm{n}^H\mathbf{T}(\theta), \tag{12}$$

which is a $P \times P$ matrix, and its dimensions are smaller than those of the transitional matrix in [11, 13].

When $P \le N - L$, $\mathbf{Q}(\theta)$ is a nonsingular matrix for a general θ since the ranks of $\mathbf{T}(\theta)$ and $\mathbf{U}_\mathrm{n}$ are P and $N - L$, respectively. However, if θ is one DOA of the incident signals, $\mathbf{Q}(\theta)$ is a singular matrix, and its determinant is zero [23]. When $\mathbf{Q}(\theta)$ is a singular matrix, we can find that Equation (11) holds and that $\mathbf{c}$ is an eigenvector of the matrix $\mathbf{Q}(\theta)$ corresponding to the eigenvalue zero, since $\mathbf{c}$ is a nonzero vector. That is to say, the degree of freedom of the proposed algorithm is $N - P$.

Namely, the mutual coupling coefficient vector $\mathbf{c}$ can be estimated by

$$\mathbf{c}_l = \frac{\mathbf{v}_{l\ \min}}{v_{l\ \min\ 1}}, \tag{13}$$

$$\widehat{\mathbf{c}} = \frac{1}{L}\sum_{l=1}^{L}\mathbf{c}_l, \tag{14}$$

where $\mathbf{v}_{l\ \min}$ denotes the eigenvector corresponding to the minimum eigenvalue of $\mathbf{Q}(\theta_l)$, and $v_{l\ \min\ 1}$ is the first entry of $\mathbf{v}_{l\ \min}$.

From Equation (12), we can find that the matrix $\mathbf{Q}(\theta_l)$ can be easily calculated by the known DOA of the incident signals, but the DOAs are unknown. Hence, we construct a new spectral function

$$P_{\det}(\theta) = \frac{1}{\det\left[\mathbf{Q}(\theta)\right]}, \tag{15}$$

where det $[\cdot]$ stands for the determinant of a matrix. Finally, $\mathbf{Q}(\theta_l)$ can be obtained through spectral peak searching since the first L peaks correspond to $\{\mathbf{Q}(\theta_l)\}_{l=1}^{L}$.

Since the noise subspace is estimated by the sampling covariance matrix, the correlation between the signal steering vector and the signal subspace improves with increasing SNR. Namely, as the SNR increases, the orthogonality of the signal and noise subspace becomes more obvious. That is, at a low SNR, the signal steering vector and the noise subspace may not be orthogonal, i.e.,

$$\mathbf{a}^H(\theta_r)\mathbf{C}^H\mathbf{U}_\mathrm{n}\mathbf{U}_\mathrm{n}^H\mathbf{Ca}(\theta_r) \neq 0, \tag{16}$$

where θ_r stands for the DOA corresponding to a signal with a low SNR.

Further, we can obtain

$$\mathbf{c}^H\mathbf{Q}(\theta_r)\mathbf{c} \neq 0. \tag{17}$$

Distinctly, $\mathbf{c}$ is not the eigenvector of the matrix $\mathbf{Q}(\theta_r)$. In other words, if there are two signals, one with a high SNR and the other with a low SNR, such as an interference signal and a desired signal simultaneously incident on an array, the estimation accuracy decreases when Equations (13) and (14) are used to estimate the mutual coupling coefficients. In this case, we can eigendecompose only $\mathbf{Q}_{\max}$ corresponding to the maximum peak of Equation (15); hence, the estimation of $\mathbf{c}$ can be given by

$$\widehat{\mathbf{c}} = \frac{\mathbf{v}_{\mathrm{m-min}}}{v_{\mathrm{m-min}\ 1}}, \tag{18}$$

where $\mathbf{v}_{\mathrm{m-min}}$ is the eigenvector corresponding to the minimum eigenvalue of the matrix $\mathbf{Q}_{\max}$, and $v_{\mathrm{m-min}\ 1}$ is the first entry of $\mathbf{v}_{\mathrm{m-min}}$.

Obviously, when multiple incident SNRs are similar, the use of Equation (18) to estimate the mutual coupling coefficients results in errors. However, in most cases, the SNRs of incident signals are not the same. For example, in RAB, due to the simultaneous existence of interference signals and the desired signal, the estimation accuracy of mutual coupling coefficients is higher when using Equation (18) than when using Equations (13) and (14).

3.2. Adaptive Beamforming with Unknown Mutual Coupling. Based on Equation (18), when there are one desired signal and L interference signals, the received data can be calibrated as

$$\begin{aligned}\widehat{\mathbf{x}}(k) = \widehat{\mathbf{C}}^{-1}\mathbf{x}(k) = \widehat{\mathbf{C}}^{-1}\mathbf{C}\left[s_0(k)\mathbf{a}(\theta_0) + \sum_{l=1}^{L}s_l(k)\mathbf{a}(\theta_l)\right] \\ + \widehat{\mathbf{C}}^{-1}\mathbf{n}(k) \approx s_0(k)\mathbf{a}(\theta_0) + \sum_{l=1}^{L}s_l(k)\mathbf{a}(\theta_l) + \widehat{\mathbf{C}}^{-1}\mathbf{n}(k).\end{aligned} \tag{19}$$

where $\widehat{\mathbf{C}} \triangleq \mathrm{Toeplitz}(\widehat{\mathbf{c}}_N, \widehat{\mathbf{c}}_N)$, $\widehat{\mathbf{c}}_N = [\widehat{\mathbf{c}}^\mathrm{T}, 0]^\mathrm{T} \in \mathbb{C}^{N\times 1}$, θ_0 is the direction of the desired signal, and $s_0(k)$ is the corresponding signal complex envelope.

Recall that in Equation (3), the covariance matrix can be rewritten as

$$\begin{aligned}\mathbf{R}_{\widehat{x}} = E\left[\widehat{\mathbf{x}}(k)\widehat{\mathbf{x}}^H(k)\right] = \sigma_0^2\mathbf{a}(\theta_0)\mathbf{a}^H(\theta_0) \\ + \sum_{l=1}^{L}\sigma_l^2\mathbf{a}(\theta_l)\mathbf{a}^H(\theta_l) + \sigma_\mathrm{n}^2\widehat{\mathbf{C}}^{-1}\widehat{\mathbf{C}}^{-H}.\end{aligned} \tag{20}$$

Distinctly, after the received data are calibrated, the noise covariance matrix is no longer $\sigma_n^2\mathbf{I}_M$ but is $\sigma_n^2\widehat{\mathbf{C}}^{-1}\widehat{\mathbf{C}}^{-H}$; namely, the white Gaussian noise becomes nonwhite Gaussian noise, which seriously affects the performance of the beamformer. Therefore, we compensate for $\mathbf{R}_{\tilde{x}}$ to obtain

$$\tilde{\mathbf{R}}_{\tilde{x}} = \widehat{\mathbf{R}}_{\tilde{x}} - \widehat{\sigma}_n^2\widehat{\mathbf{C}}^{-1}\widehat{\mathbf{C}}^{-H} + \widehat{\sigma}_n^2\mathbf{I}_M, \tag{21}$$

where $\widehat{\sigma}_n^2$ is the noise power estimate, which can be expressed as

$$\widehat{\sigma}_n^2 = \frac{1}{M-L-1}\sum_{m=L+2}^{M}\widehat{\lambda}_m, \tag{22}$$

where $\widehat{\lambda}_m$ $(m = 1, 2, \cdots, M)$ in descending order are the eigenvalues of the sample covariance matrix $\widehat{\mathbf{R}}_{\tilde{x}}$. Similarly, $\widehat{\mathbf{R}}_{\tilde{x}}$ is given by

$$\widehat{\mathbf{R}}_{\tilde{x}} = \frac{1}{K}\sum_{k=1}^{K}\widehat{\mathbf{x}}(k)\widehat{\mathbf{x}}^H(k). \tag{23}$$

Further, the INCM can be reconstructed by [24]

$$\tilde{\mathbf{R}}_{i+n} = \tilde{\mathbf{R}}_{\tilde{x}} - \widehat{\sigma}_0^2\mathbf{a}(\theta_0)\mathbf{a}^H(\theta_0) + \gamma\mathbf{I}_M, \tag{24}$$

where γ is a diagonal loading factor set to further reduce the impact of nonwhite Gaussian noise and $\widehat{\sigma}_0^2$ can be calculated as

$$\widehat{\sigma}_0^2 = \frac{1}{\mathbf{a}^H(\theta_0)\tilde{\mathbf{R}}_{\tilde{x}}^{-1}\mathbf{a}(\theta_0)}. \tag{25}$$

Under the minimum variance distortionless response principle for RAB, the weight vector is usually expressed as [25]

$$\mathbf{w}_{\text{opt}} = \frac{\mathbf{R}_{i+n}^{-1}\mathbf{a}(\theta_0)}{\mathbf{a}^H(\theta_0)\mathbf{R}_{i+n}^{-1}\mathbf{a}(\theta_0)}, \tag{26}$$

where $\mathbf{R}_{i+n}$ denotes the ideal INCM without mutual coupling.

Using $\tilde{\mathbf{R}}_{i+n}$ in lieu of $\mathbf{R}_{i+n}$ yields

$$\widehat{\mathbf{w}}_{\text{opt}} = \frac{\tilde{\mathbf{R}}_{i+n}^{-1}\mathbf{a}(\theta_0)}{\mathbf{a}^H(\theta_0)\tilde{\mathbf{R}}_{i+n}^{-1}\mathbf{a}(\theta_0)}. \tag{27}$$

However, Equation (11) cannot be used to estimate the MCM when$M - L - 1 < P$, since $\mathbf{Q}(\theta)$ is a singular matrix for any θ. Namely, the DOF of the proposed algorithm is limited for a fixed ULA.

The main computational load of the designed beamformer is caused by estimating mutual coupling coefficients. The process of estimating mutual coupling coefficients consists of two parts: one is the construction of spectral function, and the other is the search of spectral peaks. Hence, the computational load of the proposed method is approximately $O(M^3) + S \times O(P^3)$, where $O(M^3)$ is due to the construction of spectral function, $S \times O(P^3)$ is caused by the search of spectral peaks, and S is the number of spectral peak searches.

In other words, the proposed beamformer can be summarized as follows:

Step 1. Estimate the covariance matrix $\mathbf{R}_{\tilde{x}}$ using Equation (4), and eigendecompose it using Equation (5).

Step 2. Construct the transformation matrix and the transitional matrix using Equations (7) and (12), respectively.

Step 3. Estimate the transitional matrix $\mathbf{Q}_{\max}$ corresponding to the highest SNR signal by searching for the highest peak of Equation (15), and estimate the mutual coupling coefficient vector using Equation (18).

Step 4. Reconstruct the INCM by calibrating the received data and compensating for calibration errors using Equation (24).

Step 5. Calculate the weight using Equation (27).

4. Simulations

In this section, we implement several simulations to validate the effectiveness and superiority of the proposed algorithm. A ULA with $N = 12$ elements spaced a half-wavelength apart is used. The additive noise in the elements is modeled as spatially and temporally independent complex Gaussian noise with zero mean and unit variance. We assume that the mutual coupling coefficient vector is

$$\mathbf{c} = \left[1, 0.90e^{-j\pi/3}, 0.75e^{j\pi/4}, 0.45e^{-j\pi/10}, 0.15e^{-j\pi/6}\right]^T. \tag{28}$$

According to the previous analysis, an iterative algorithm and two subspace-based methods without iteration are selected for comparison, and the three algorithms are called Liao's method [14], Elbir's method [18], and Wen's method [20]. In each trial, the number of angular sectors is selected as 12, and $\varepsilon = 10^{-4}$ in Elbir's method. In addition, the Cramér-Rao bound (CRB) of the real and imaginary parts of the mutual coupling coefficients is provided in simulations. Note that the calculation of CRB is performed as in [26], and the CRB is modified to correspond to the real and imaginary parts of the mutual coupling coefficients.

Example 1. The directions of the desired signal and two interferences are assumed to be 10°, -20°, and 40°, respectively, and the corresponding SNR and interference-to-noise ratio (INR) are set to 10 dB and 40 dB, respectively. The number of snapshots is 500, and 100 Monte Carlo runs are performed. In this experiment, the results of the estimation of mutual coupling coefficients are listed in Table 1 (a single run). The proposed method successfully estimates all mutual coefficients with high accuracy. Figure 1 displays the root mean square error (RMSE) of the real and imaginary parts of all mutual coupling coefficients versus SNR and the number of snapshots, where the RMSE is calculated by

$$\text{RMSE} = \sqrt{\frac{1}{M(P-1)}\sum_{m=1}^{M}\sum_{p=1}^{P-1}\left(\widehat{w}_m^p - w^p\right)^2}, \tag{29}$$

Table 1: Mutual coupling coefficient estimation (SNR = 10 dB).

Mutual coupling coefficients	Real part (α)		Imaginary part (β)	
	$\widehat{\alpha}$	α	$\widehat{\beta}$	β
c_1	0.4488	0.4500	-0.7766	-0.7794
c_2	0.5288	0.5303	0.5284	0.5303
c_3	0.4264	0.4280	-0.1392	0.1391
c_4	0.1303	0.1299	-0.0742	-0.0750

where M is the number of Monte Carlo runs, w^p denotes the real or imaginary part of c_p, and $\widehat{w}_m^p$ stands for the estimated value of w^p in the mth trial.

Figure 1(a) displays the RMSE values of the estimation of the real and imaginary parts of all the mutual coupling coefficients versus the SNR. The RMSE of the real and imaginary parts of all the mutual coupling coefficients versus the number of snapshots is shown in Figure 1(b). As we can see, the mutual coupling coefficient estimation accuracy of the proposed algorithm is always close to the CRB; when the difference in the signal power is large, the performance of the proposed method is closer to the CRB, and the larger the difference is, the more obvious the advantage of the proposed algorithm. However, when the power of each signal is similar, the performance of the proposed method is worse than that of Liao's method and Wen's algorithm but is still better than that of Elbir's algorithm. These results occur because when all the signal powers are similar, the mutual coupling coefficients estimated by all the transitional matrices are close to each other, and the mutual coupling coefficients obtained using more information have higher accuracies. Additionally, when the SNR of the desired signal is significantly higher than the INR of the interference signal, the proposed method still yields better performance.

Example 2. The performance of the proposed beamformer and several classical robust adaptive beamformers, such as LSMI, MSB, MSRB, and SRB, is investigated in this example. In addition, the simulation compares a simplified SRB (SSRB) beamformer obtained utilizing Wen's method to replace the mutual coupling coefficient estimation algorithm in the SRB beamformer. The output signal-to-interference-plus-noise ratio (SINR) versus the SNR with the number of snapshots fixed at 500 and the output SINR versus the number of snapshots with the SNR fixed at 10 dB are analyzed. Figure 2(a) displays the output SINR of different beamformers versus SNR, while Figure 2(b) shows the output SINR of those approaches versus the number of snapshots.

In Figure 2, the output SINR of the proposed beamformer is always close to the optimal SINR. In addition, at a high SNR, its performance is close to that of the SRB beamformer and SSRB beamformer, which is obviously better than that of the other algorithms. However, at a low SNR, the performance of the designed beamformer is obviously higher than that of the SRB beamformer and the SSRB beamformer due to the high-precision estimation of the mutual coupling matrix. The performance of the MSRB beamformer is limited by the array aperture and is always lower than that of the proposed beamformer. In addition, the designed beamformer has a faster convergence rate than the SRB beamformer and SSRB beamformer and is always close to the optimal output SINR.

Example 3. The performance of the designed beamformer with the unknown direction error is analyzed in this example. It is assumed that there is a random direction error of the desired signal, and it is uniformly distributed in $[-2^\circ, 2^\circ]$ in each trial. Namely, the direction error of the desired signal changes from run to run but remains fixed in one trial. The results are shown in Figure 3.

Compared with Figure 2, the performance of the proposed beamformer, the SRB beamformer, and the SSRB beamformer is basically unchanged in Figure 3 because these three beamformers can estimate the desired signal direction when estimating the mutual coupling coefficients. The performance of the MSRB beamformer is only slightly degraded, but that of the MSB beamformer is seriously degraded because INCM reconstruction is utilized in the MSRB beamformer but not in the latter. Note that the convergence rate of the proposed beamformer is also very fast compared to those of other beamformers.

Example 4. The performance of the designed beamformer with incoherent local scattering.

The influence of incoherent local scattering is considered in this experiment. Generally, incoherent local scattering always occurs and seriously affects the performance of the beamformer. Here, we assume that in the case of incoherent local scattering, the received desired signal can be expressed as

$$\mathbf{x}_s(k) = \mathbf{a}(\theta_0)s_0(k) + \sum_{q=1}^{3} s_q(k)\mathbf{a}(\theta_q), \tag{30}$$

where $\theta_q (q = 1, 2, 3)$ denotes the direction of the qth local scattering signal and is subject to uniform distribution in $[\theta_0 - 2^\circ, \theta_0 + 2^\circ]$ and $s_q(k)$ and $\mathbf{a}(\theta_q)$ are the corresponding signal waveform and the steering vector, respectively. The simulation results are shown in Figure 4.

Figure 4 displays the simulation result of each tested beamformer with incoherent local scattering. Compared with Figure 2, since local scattering signals disturb the sampling covariance matrix, the performance of all tested beamformers deteriorates to varying degrees, especially at high SNRs. Since the incoherent scattering signal causes serious errors in the estimation of the mutual coupling coefficient at a high SNR, the performance of all algorithms is seriously degraded at a high SNR. However, at a low SNR, the influence of the incoherent scattered signal is small, and the proposed algorithm only utilizes the highest power signal to estimate mutual coupling coefficients; thus, the performance of the proposed beamformer is always close to the optimal output SINR. In addition, the convergence rate of

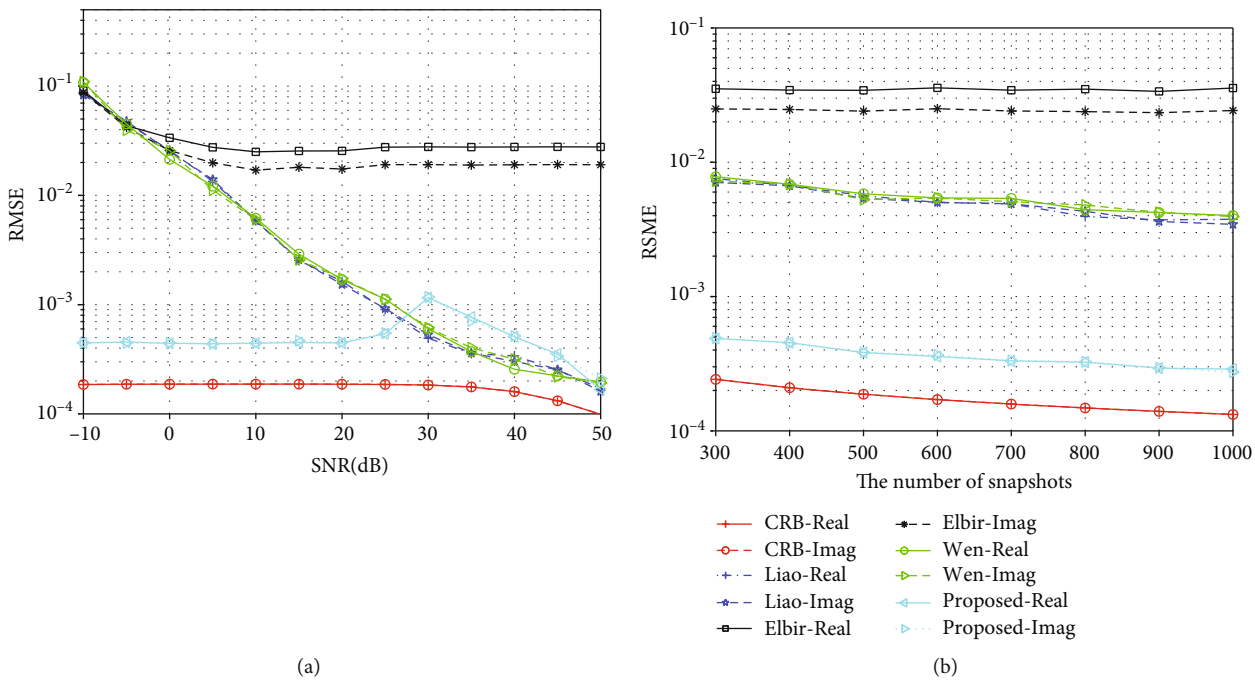

Figure 1: (a) RMSE of the mutual coupling coefficients versus SNR, $K = 500$, INR = 40 dB. (b) RMSE of the mutual coupling coefficients versus the number of snapshots, SNR = 10 dB, INR = 40 dB.

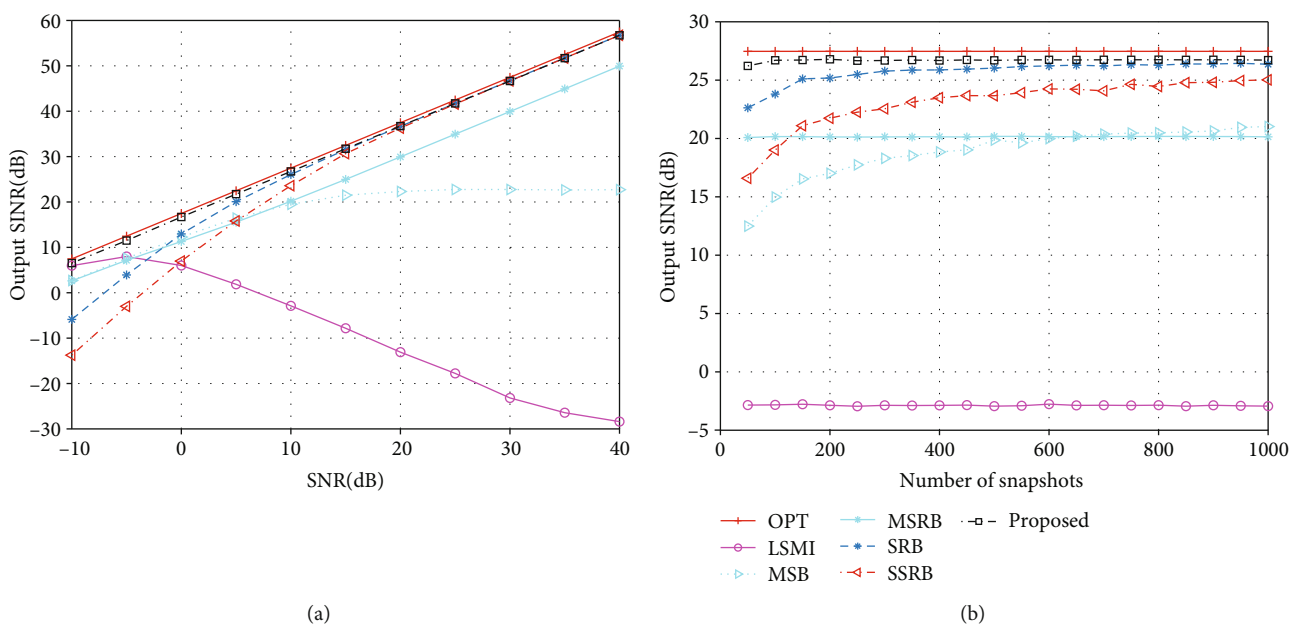

Figure 2: (a) Output SINR versus SNR, INR = 40 dB, $K = 500$. (b) Output SINR versus the number of snapshots, SNR = 10 dB, INR = 40 dB.

the proposed beamformer is very fast compared to those of other beamformers.

5. Conclusion

In this paper, a modified subspace-based mutual coupling coefficient estimation algorithm for beamforming is proposed. The main contribution of this manuscript includes two parts: (1) to improve the mutual coupling coefficient estimation accuracy, we propose a strategy to improve the estimation accuracy by choosing appropriate transition matrices; (2) to improve the robustness of the beamformer to unknown mutual coupling, a beamformer is designed combining the calibrated steering vector and the interference-plus-noise covariance matrix reconstruction method. The proposed beamformer has superior performance than exiting algorithms especially when there is a big power gap between different interferences. Simulations demonstrate

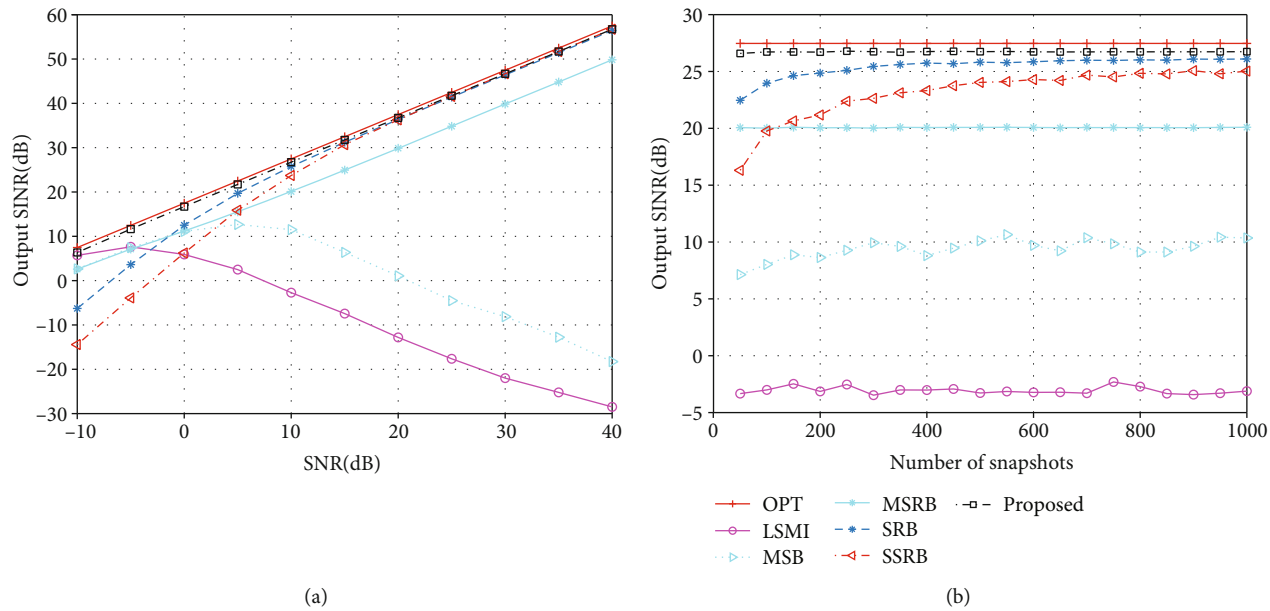

Figure 3: (a) Output SINR versus SNR with the unknown direction error, INR = 40 dB, $K = 500$. (b) Output SINR versus the number of snapshots with the unknown direction error, SNR = 10 dB, INR = 40 dB.

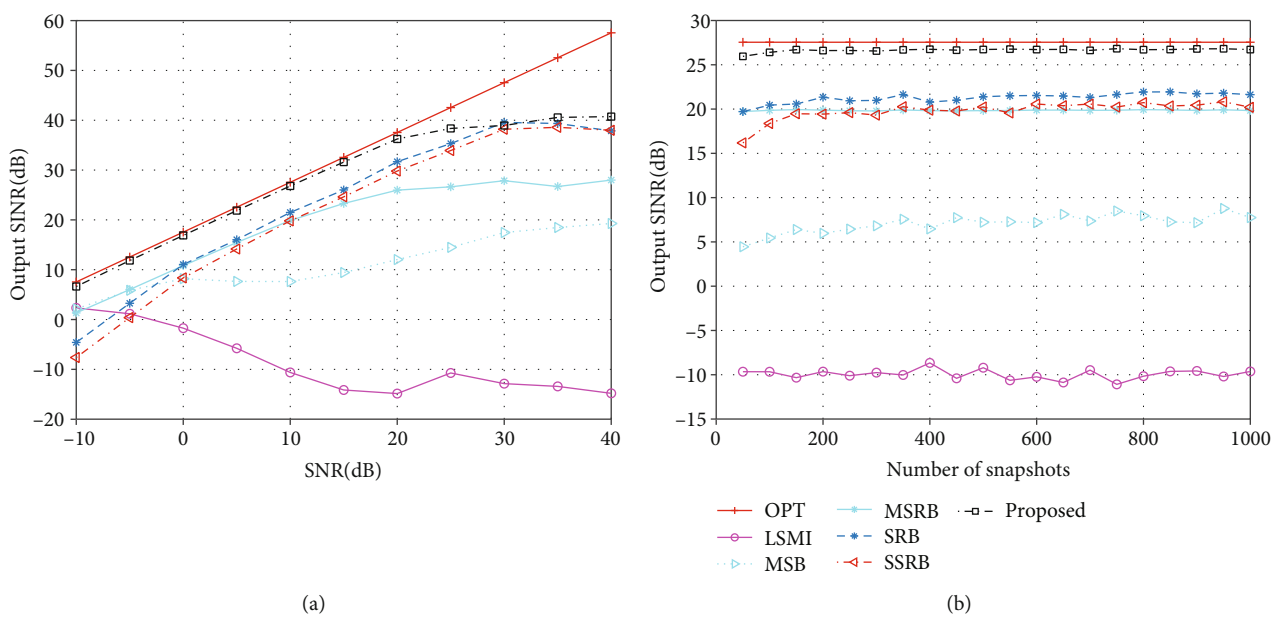

Figure 4: (a) Output SINR versus SNR with incoherent local scattering, INR = 40 dB, $K = 500$. (b) Output SINR versus the number of snapshots with incoherent local scattering, SNR = 10 dB, INR = 40 dB.

the superiority of the modified subspace-based mutual coupling coefficient estimation algorithm and the robustness of the designed beamformer to unknown mutual coupling.

Data Availability

The data sources from the references are all marked in this paper. And the parameters designed are all described in this paper. Therefore, the data in this paper has been fully covered and can be obtained.

Conflicts of Interest

The authors declare that they have no conflicts of interest.

Acknowledgments

This work is supported in part by the National Natural Science Foundation of China (Grants 61901511 and 61871471), in part by the National Science Foundation of Shaanxi Province of China (Grant 2019JM-322), in part by the Natural Science Basic Research Plan in Shaanxi Province of China (Grant

2020JQ-478), and in part by the Research Program of the National University of Defense Technology (Grant ZK19-10).

References

[1] W. Zhang and S. A. Vorobyov, "Joint robust transmit/receive adaptive beamforming for MIMO radar using probability-constrained optimization," *IEEE Signal Processing Letters*, vol. 23, no. 1, pp. 112–116, 2016.

[2] S. D. Somasundaram, "Wideband robust Capon beamforming for passive sonar," *IEEE Journal of Oceanic Engineering*, vol. 38, no. 2, pp. 308–322, 2013.

[3] Z. Xiang and M. Tao, "Robust beamforming for wireless information and power transmission," *IEEE Wireless Communications Letters*, vol. 1, no. 4, pp. 372–375, 2012.

[4] L. Wan, X. Kong, and F. Xia, "Joint range-Doppler-angle estimation for intelligent tracking of moving aerial targets," *IEEE Internet of Things Journal*, vol. 5, no. 3, pp. 1625–1636, 2018.

[5] F. Wen and J. Shi, "Fast direction finding for bistatic EMVS-MIMO radar without pairing," *Signal Processing*, vol. 173, article 107512, p. 107512, 2020.

[6] J. Shi, F. Wen, and T. Liu, "Nested MIMO radar: coarrays, tensor modeling and angle estimation," *IEEE Transactions on Aerospace and Electronic Systems*, 2020.

[7] X. Wang, L. Wang, X. Li, and G. Bi, "Nuclear norm minimization framework for DOA estimation in MIMO radar," *Signal Process*, vol. 135, pp. 147–152, 2017.

[8] B. Friedlander and A. Weiss, "Direction finding in the presence of mutual coupling," *IEEE Transactions on Antennas and Propagation*, vol. 39, no. 3, pp. 273–284, 1991.

[9] J. Dai, X. Bao, N. Hu, C. Chang, and W. Xu, "A recursive RARE algorithm for DOA estimation with unknown mutual coupling," *IEEE Antennas and Wireless Propagation Letters*, vol. 13, pp. 1593–1596, 2014.

[10] Z. Zheng, K. Liu, W.-Q. Wang, Y. Yang, and J. Yang, "Robust adaptive beamforming against mutual coupling based on mutual coupling coefficients estimation," *IEEE Transactions on Vehicular Technology*, vol. 66, no. 10, pp. 9124–9133, 2017.

[11] B. Liao and S.-C. Chan, "Adaptive beamforming for uniform linear arrays with unknown mutual coupling," *IEEE Antennas and Wireless Propagation Letters*, vol. 11, pp. 464–467, 2012.

[12] Z. Ye and C. Liu, "Non-sensitive adaptive beamforming against mutual coupling," *IET Signal Processing*, vol. 3, no. 1, pp. 1–6, 2009.

[13] Z. Zheng, W.-Q. Wang, Y. Kong, and Y. D. Zhang, "MISC array: a new sparse array design achieving increased degrees of freedom and reduced mutual coupling effect," *IEEE Transactions on Signal Processing*, vol. 67, no. 7, pp. 1728–1741, 2019.

[14] B. Liao, Z.-G. Zhang, and S.-C. Chan, "DOA estimation and tracking of ULAs with mutual coupling," *IEEE Transactions on Aerospace and Electronic Systems*, vol. 48, no. 1, pp. 891–905, 2012.

[15] B. Liao and S.-C. Chan, "A cumulant-based method for direction finding in uniform linear arrays with mutual coupling," *IEEE antennas and wireless propagation letters*, vol. 13, pp. 1717–1720, 2014.

[16] M. Wang, X. Ma, S. Yan, and C. Hao, "An autocalibration algorithm for uniform circular array with unknown mutual coupling," *IEEE Antennas and Wireless Propagation Letters*, vol. 15, pp. 12–15, 2015.

[17] F. Wen, Z. Zhang, K. Wang, G. Sheng, and G. Zhang, "Angle estimation and mutual coupling self-calibration for ULA-based bistatic MIMO radar," *Signal Processing*, vol. 144, pp. 61–67, 2018.

[18] A. M. Elbir, "Direction finding in the presence of direction-dependent mutual coupling," *IEEE Antennas and Wireless Propagation Letters*, vol. 16, pp. 1541–1544, 2017.

[19] Q. Ge, Y. Zhang, and Y. Wang, "A low complexity algorithm for direction of arrival estimation with direction-dependent mutual coupling," *IEEE Communications Letters*, vol. 24, no. 1, pp. 90–94, 2019.

[20] F. Wen, J. Wang, J. Shi, and G. Gui, "Auxiliary vehicle positioning based on robust DOA estimation with unknown mutual coupling," *IEEE Internet of Things Journal*, vol. 7, no. 6, pp. 5521–5532, 2020.

[21] Y. Gu and A. Leshem, "Robust adaptive beamforming based on interference covariance matrix reconstruction and steering vector estimation," *IEEE Transactions on Signal Processing*, vol. 60, no. 7, pp. 3881–3885, 2012.

[22] Z. Li, Y. Zhang, Q. Ge, and Y. Guo, "Middle subarray interference covariance matrix reconstruction approach for robust adaptive beamforming with mutual coupling," *IEEE Communications Letters*, vol. 23, no. 4, pp. 664–667, 2019.

[23] C. M. S. See and A. B. Gershman, "Direction-of-arrival estimation in partly calibrated subarray-based sensor arrays," *IEEE Transactions on Signal Processing*, vol. 52, no. 2, pp. 329–338, 2004.

[24] S. A. Vorobyov, "Principles of minimum variance robust adaptive beamforming design," *Signal Processing*, vol. 93, no. 12, pp. 3264–3277, 2013.

[25] Z. Zheng, T. Yang, W.-Q. Wang, and H. C. So, "Robust adaptive beamforming via simplified interference power estimation," *IEEE Transactions on Aerospace and Electronic Systems*, vol. 55, no. 6, pp. 3139–3152, 2019.

[26] M. Wang and A. Nehorai, "Coarrays, MUSIC, and the Cramér-Rao bound," *IEEE Transactions on Signal Processing*, vol. 65, no. 4, pp. 933–946, 2017.